Quantum well band formation in Ag films on InSb(111)

2009 J. Phys.: Condens. Matter 21 355502

(http://iopscience.iop.org/0953-8984/21/35/355502)

J. Phys.: Condens. Matter **21** (2009) 355502 (5pp) doi:10.1088/0953-8984/21/35/355502

Quantum well band formation in Ag films on InSb(111)

P Moras and C Carbone

Istituto di Struttura della Materia, Consiglio Nazionale delle Ricerche, Trieste, Italy

Received 21 April 2009
Published 11 August 2009
Online at stacks.iop.org/JPhysCM/21/355502

Abstract

Room temperature deposition of Ag on InSb(111) is known to lead to three-dimensional clustering, without long-range crystalline order. We show by means of angle-resolved photoemission that 'two-step' growth in which the films are annealed to room temperature after low temperature deposition results in the formation of Ag films which are epitaxial, atomically flat, and display a quasi-discrete quantum well band structure. Core level analysis highlights different chemical interactions between the substrate and deposited materials for room temperature and 'two-step' Ag growth.

(Some figures in this article are in colour only in the electronic version)

For technological and fundamental purposes it is usually desirable to produce sharp interfaces and crystalline films, by properly devising the growth procedure. The growth mode of a film can be predicted, to a first approximation, as a result of the balance between the surface energies and the adhesion energy of the substrate and adsorbed materials [1]. However, the formation of metal–semiconductor interfaces is generally complicated by chemical reactions and atomic interdiffusion occurring among the chemical species. Under typical condition the interface morphology, film structure, and composition are influenced by kinetic limits, with the atomic mobility and, consequently, the temperature playing a key role.

In recent years it has been observed that the so-called 'two-step' technique allows to grow films of metallic elements in a layer-by-layer fashion on different substrates [2–5]. In the first step the metal is evaporated on the substrate, kept at a sufficiently low temperature in order to limit the atomic mobility and to hinder clustering. A gradual annealing to room temperature (second step) promotes the film crystallization, with completion of atomically flat regions of mesoscopic areas (thousands of nm^2). The 'two-step' procedure is exploited for the growth of films with very uniform thickness which exhibit quantum size electronic effects [6]. The film thickness defines the spatial width of a two-dimensional potential well for the electron wave functions and, consequently, determines the energy spectrum of quantum well (QW) states. The realization of discrete QW bands enhances observable macroscopic properties related to the electron confinement in two dimensions. Atomically flat films present size dependent effects which finely modulate the surface chemical reactivity [7], the superconducting critical temperature [8], the magnetic state in multilayer structures [9], and other properties, which can be tuned by precise control of the thickness.

Among the different classes of metal films, Ag layers represent simple model systems, because of their limited reactivity, noble metal character, and relatively low surface free energy. The effects of the 'two-step' growth have been examined with different degree of success on several semiconductor surfaces. Ag layers display a very well defined quantum well structure on Ge(111) [10, 11], Si(111) [12, 13], and Si(100) [12, 14], on which they form sharp interfaces. Flat Ag films, above a critical thickness, have been also obtained on several III–V semiconductor (110) surfaces, i.e. GaAs, GaP, GaSb, InAs, InP, and InSb [15]. The low energy electron diffraction (LEED) pattern and STM pictures indicate, however, a tendency to produce distorted or modulated (111)-films, with QW states formation established only on GaAs [16–18].

On the other side, the tendency to intermix and react appears to be an obstacle to the successful application of the 'two-step' growth for QW formation. It is known that Ag forms reacted interfaces when deposited at room temperature on several In–V semiconductors [19]. On InSb(110), for example, the 'two-step' method produces a weak (111)-pattern for a Ag thickness of 35 Å [15], indicating a significant amount of structural disorder. A QW state could be observed for Ag on InSb(110) only for thin films of 3.8 monolayers [20]. The exploitation of quantum design of the electronic properties in this class of systems appears to require better control of the

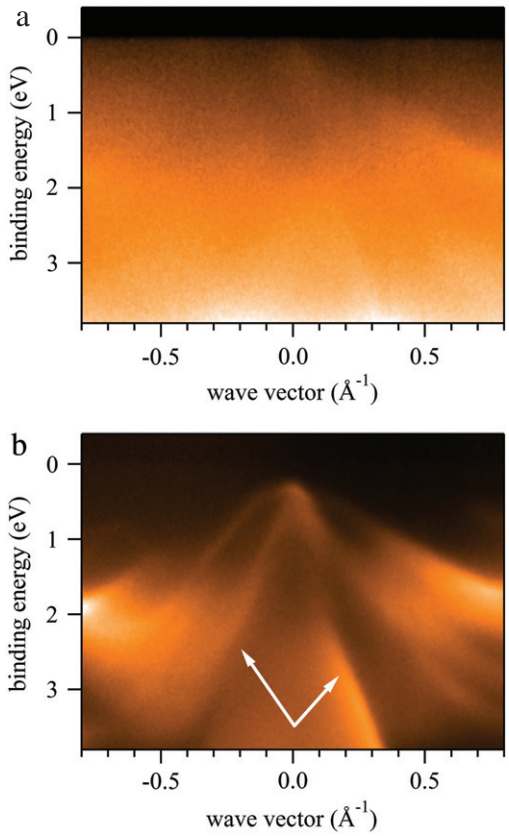

Figure 1. Angle-resolved photoemission maps acquired at 45 eV photon energy for (a) 42.5 Å Ag film deposited at room temperature and (b) the bare InSb(111)-(2 × 2) measured along the $\bar{\Gamma}$–$\bar{K}$ substrate direction.

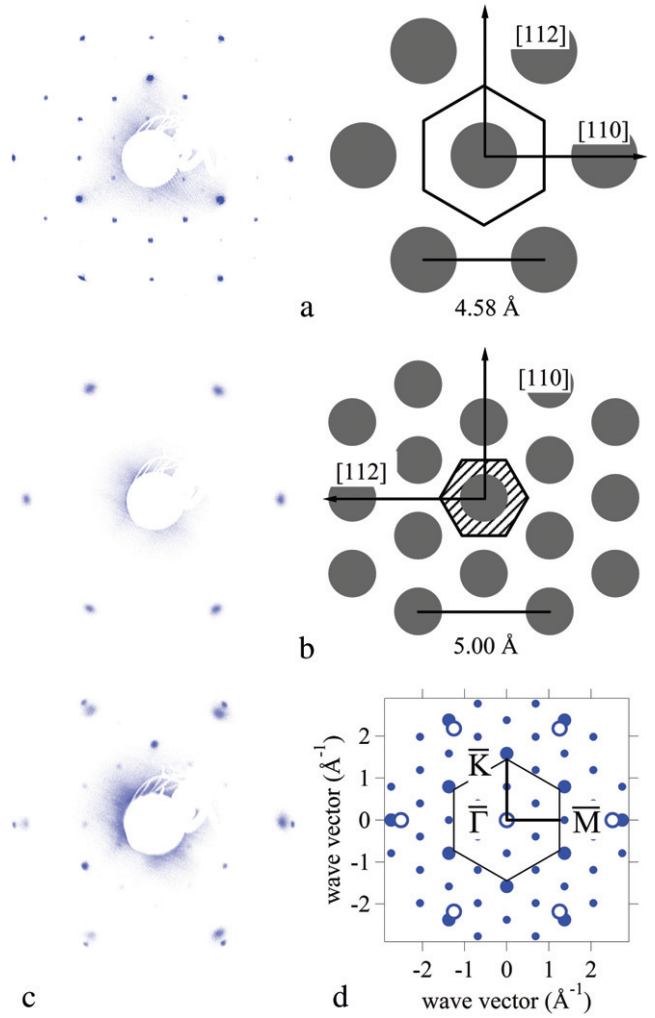

Figure 2. LEED patterns observed on (a) the clean InSb(111)-(2 × 2) substrate, (b) the 42.5 Å (18 ML) Ag film grown following the 'two-step' procedure, and (c) the edge between bare and Ag covered parts of the sample. Evidently, panel (c) is the sum of the patterns shown in (a) and (b), and allows a direct comparison of the structural parameters of substrate and film. (d) Scheme of the LEED pattern derived from panel (c), where open circles refer to Ag spots and full circles represent the 1× (big symbols) and 2× (small symbols) periodicity of the substrate. The first surface Brillouin zone and symmetry points of the Ag(111) film are also shown. The bulk truncated atomic structures of InSb(111) and Ag(111) planes are reported on the right-hand side of panels (a) and (b), respectively.

chemical and structural uniformity in order to ensure sufficient lateral coherence of the surface and interface electronic potentials.

In this work we compare the electronic structure and growth mode of Ag films grown on InSb(111) by the 'two-step' and room temperature deposition, to explore the potential of different growth procedures on reactive interfaces with respect to the realization of distinct quantum structures. In agreement with previous investigations, both indium and antimony are found to form a disordered alloy when Ag is deposited at room temperature [21]. In contrast with the room temperature deposition and with the Ag growth on InSb(110) [15, 20], the 'two-step' growth on InSb(111) gives rise to ordered crystalline layers, with a flat surface and a defined QW band structure for relatively thick films. Different chemical interaction and structural relations appear to be related to the diverse growth mode and electronic properties of Ag films on InSb substrates.

The experiments were carried out at the VUV-Photoemission beam line on the synchrotron Elettra in Trieste. The n-type wafers of InSb(111) were cleaned *in situ* by repeated cycles of sputtering with Ar ions (800 eV) and annealing (700 K). This procedure gives rise to contaminant free surfaces with a (2 × 2) LEED pattern, explained in terms of the In-vacancy buckling model [22]. Ag was deposited from a resistively heated crucible, whose evaporation rate was determined with a quartz microbalance and cross checked with photoemission. The 'two-step' growth was performed with the sample held at 140 K and warmed up to room temperature. The photoemission data were acquired with a Scienta R-4000 electron analyzer, which allows parallel acquisition of angle-resolved spectra over 30° emission angle.

We choose to compare the properties of fairly thick (42.5 Å, corresponding to 18 ML, 1 ML = 2.36 Å) Ag films obtained through direct deposition at room temperature and by the 'two-step' growth mode. The deposition of Ag on the InSb(111) surface at room temperature gives results similar to those obtained for Ag layers on other III–V semiconductors, such as InP(110) and InSb(110) [19]. The diffraction pattern

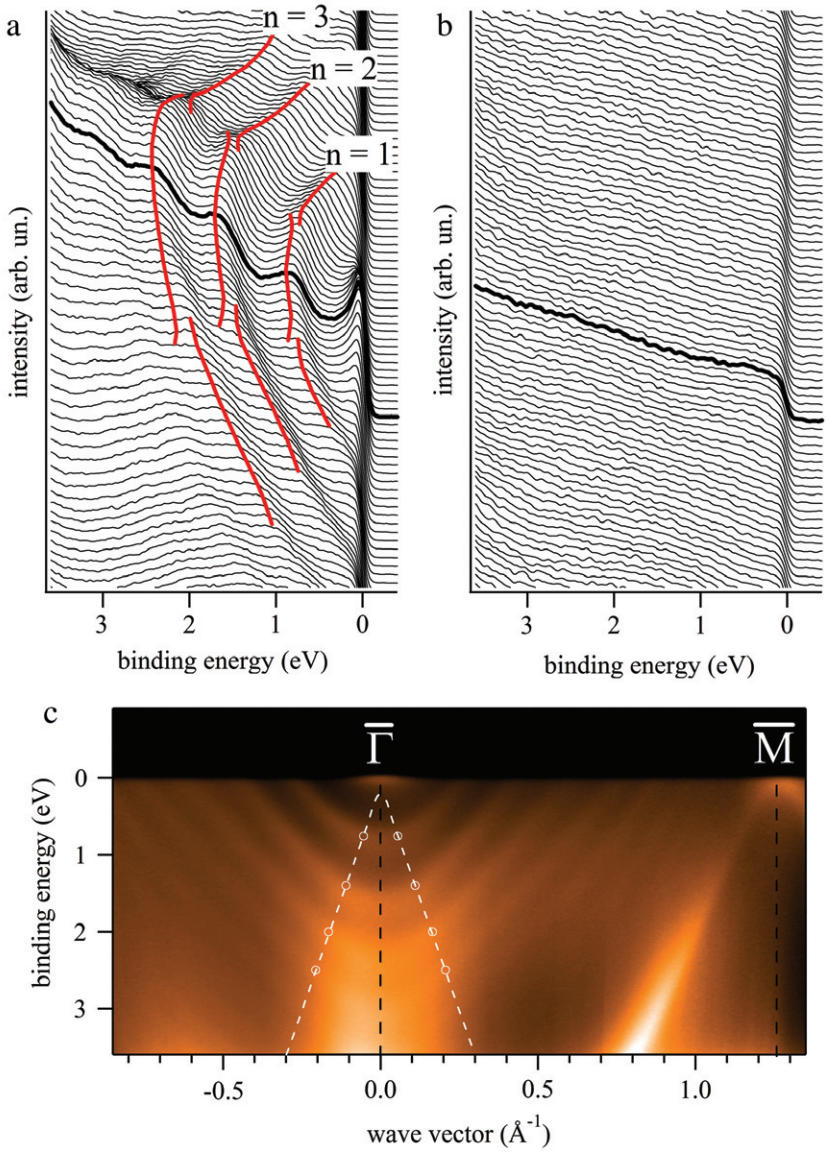

Figure 3. Angle-resolved spectra for 42.5 Å Ag films grown following (a) the 'two-step' and (b) the room temperature deposition procedure, measured over the same angle and energy range along the $\bar{\Gamma}$–$\bar{M}$ direction of Ag(111). Panel (c) reports a photoemission intensity map for the 42.5 Å Ag film grown following the 'two-step' method. The open circles indicate the location of the discontinuities (gaps) observed along the QW bands.

is totally absent. The angle-resolved photoemission map of this system (figure 1(a)), measured along the $\bar{\Gamma}$–$\bar{K}$ direction of the substrate at 45 eV photon energy, is almost featureless, apart from very weak bands which display a downward dispersion from normal emission angle. These bands derive from the substrate electronic structure, as demonstrated by comparison with the photoemission map of the InSb(111) surface (figure 1(b)). As already noticed in [21], Ag deposited at room temperature forms three-dimensional islands separated by bare or little covered portions of the semiconductor surface, from which the substrate electronic states can be detected in the photoemission measurement.

These findings strikingly contrast with the properties of Ag films deposited according to the 'two-step' procedure. Figure 2 shows the LEED patterns for 51 eV primary electron energy. The clean surface in panel (a) presents a (2 × 2) reconstruction. Panel (b) reports the diffraction pattern for the Ag film deposited at low temperature, after the sample has reached room temperature. The relationship between the patterns displayed in panel (a) and (b) can be directly derived from figure 1(c). This picture was acquired with the primary electron beam positioned across the edge between the clean and Ag covered parts of the sample (half of the sample surface was purposely masked with a shutter during the deposition). The lattice parameters of the Ag film can be evaluated by comparison with the known size of the substrate pattern. The Ag first order spots fall in the vicinity of the second rim of integer spots of the substrate and their separation closely corresponds to the Ag bulk truncated value along a (111) plane. Hence, within the first surface Brillouin zone of Ag(111), the $\bar{\Gamma}$–$\bar{M}$ axis of the film runs parallel to the $\bar{\Gamma}$–$\bar{K}$ axis of the substrate, and vice versa, as displayed in figure 1(d).

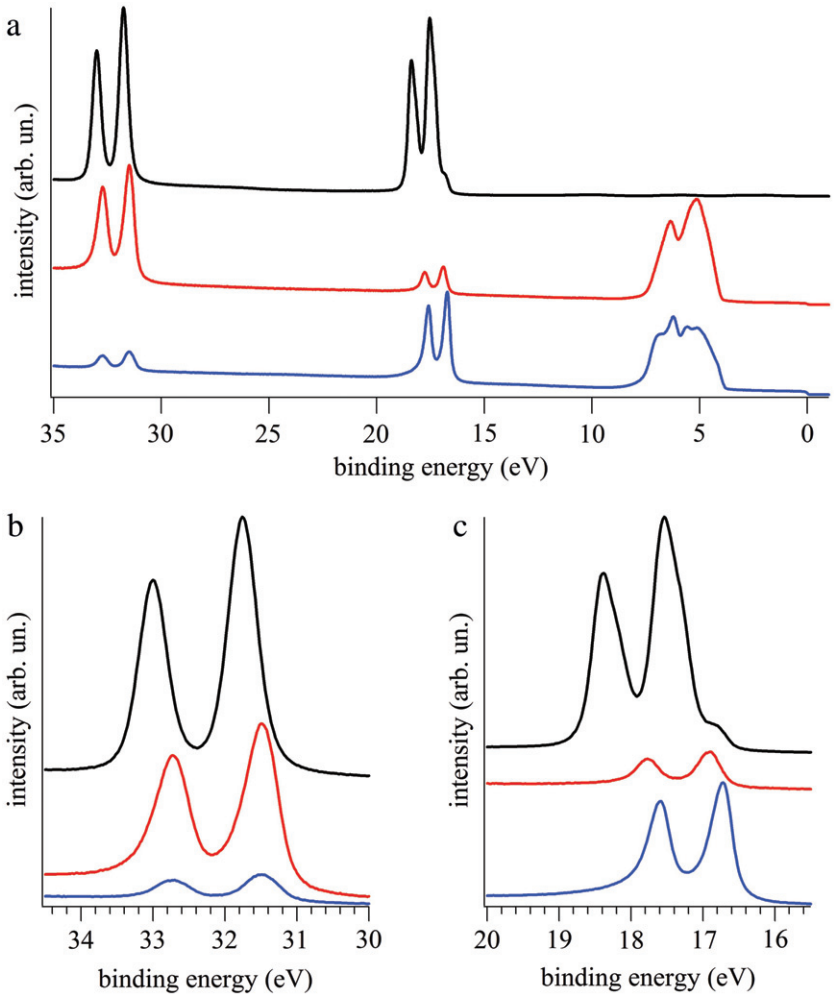

Figure 4. Angle-integrated spectra for the clean (top) and 42.5 Å Ag films deposited at room temperature (middle) and low temperature (bottom). Panel (a) reports a wide energy scan. Panels (b) and (c) display more in detail the Sb 4d and In 4d core level line shapes of the systems.

In order to elucidate the relationship between film and substrate structures in real space, we draw the atomic arrangement of InSb(111) and Ag(111) lattice planes on the right-hand side of figures 2(a) and (b), respectively. For InSb the circles may represent either indium or antimony atoms. The Wigner–Seitz cells in both cases are hexagons, rotated in-plane by 90° with respect to each other, so that the $[11\bar{2}]$ surface axis of Ag runs parallel to the $[1\bar{1}0]$ surface axis of InSb. The observed growth is possibly favored by the similar value of the nearest neighbor distance in the InSb(111) plane (4.58 Å) and the second nearest neighbor distance in the Ag(111) plane (5.00 Å), in spite of a 9.1% mismatch.

Figure 3(a) reports a set of angle-resolved photoemission spectra for the film obtained through the 'two-step' growth and acquired at 45 eV photon energy along the $\bar{\Gamma}$–$\bar{M}$ direction. The data display a series of QW states, whose binding energy diminishes as the electron emission angle is increased (the thickest line corresponds to the spectrum measured in normal emission geometry). These peaks can be labeled with integer quantum numbers $n = 1, 2, 3, \ldots$, according to the nomenclature conventionally adopted for Ag(111) films [6]. The additional peak lying close to the Fermi edge in the near normal emission region is attributed to the Ag(111) surface state. The observed QW band structure is a clear mark of thickness uniformity, as well as of the existence of a sufficiently uniform confining potential barrier for the Ag sp-electrons at the interface. At a closer inspection the QW state dispersion appears to be characterized by several weak discontinuities. The lines drawn on the peak maxima in figure 3(a) help to identify their position and the size of the corresponding gaps. In contrast with these findings, the valence band of Ag films directly prepared at room temperature is almost unstructured (figure 3(b)). The modulation of the photoemission signal due to quantum confinement effects is completely absent as well as the Ag(111) surface state.

A wider set of data than that shown in figure 3(a) was used to generate the photoemission intensity map of figure 3(c). In this image the QW states exhibit a nearly parabolic band dispersion with minima centered around the $\bar{\Gamma}$ point. The overall behavior of the *sp*-derived QW states agrees with previous findings for related systems, such as Ag films on Ge(111) [10, 11] and Si(111) [12, 13]. The above

mentioned discontinuities, whose positions are marked with open circles in the intensity map, are features commonly found in the electronic structure of epitaxial metal films grown on semiconductors [4]. These gaps originate from the symmetry dependent hybridization between film and substrate states. In photoemission experiments they become particularly evident when the QW states cross the upper edges of the surface projected bands of the semiconductor [10]. In the present case the gaps define a curve in the energy-wavevector space which follows the downward dispersion of the InSb bands highlighted with arrows in figure 1(b). The intensity of the Ag(111) surface state in the present case is weaker than for related systems measured within the same photon energy range.

Additional information on the different atomic structure of the systems can be derived from core level spectroscopy. Figure 4 reports angle-integrated spectra acquired at 71.5 eV photon energy in normal emission geometry. For each panel the black (top) spectrum refers to the InSb surface, while red (middle) and blue (bottom) spectra correspond to room and low temperature depositions of 42.5 Å Ag, respectively. Panel (a) presents wide energy scans, covering the Sb 4d, In 4d and valence regions. Panels (b) and (c) report more in detail the Sb 4d and In 4d lines.

The Sb 4d/In 4d ratios are markedly dissimilar for the two Ag covered samples. The results for the system grown at room temperature are in agreement with other reports on Ag on InSb(111). The Ag growth at room temperature proceeds in a Stransky–Krastanov mode with alloy formation more Sb than In rich in the outer layers [21], as confirmed in figure 4(a) by the different attenuation of the two core levels. A similar growth also occurs for Ag on InSb(110). The energy shift and line shape of the Sb 4d states are, consistently, signs of Sb atoms included in a metallic alloy. For the sample prepared according to the 'two-step' procedure, instead, we find an enhanced segregation of the In atoms to the surface, as indicated by the angular dependence of the core level emission (not shown). This behavior, occurring despite the kinetic limitation of the growth process, deserves further microscopic and spectroscopic analysis. Anyway, the selective surface segregation of indium can explain the experimental observations, i.e. the relatively intense In 4d peaks, the reversed Sb 4d/In 4d ratio, and the weakness of the Ag(111) surface state. The low Sb 4d signal indicates a suppressed, but not negligible degree of intermixing with Ag at the interface.

In conclusion, we find that quantum structures can be produced on a reactive interface by applying a proper growth procedure. The 'two-step' growth significantly alters the properties of Ag films on InSb(111) and limits the interdiffusion. It promotes crystalline growth of Ag films and formation of mesoscopic areas with atomically uniform height. The films present the characteristics of a two-dimensional quantum structure with discrete electronic bands, weakly modified by the hybridization with the substrate electronic states.

References

[1] Bauer E and Poppa H 1972 *Thin Solid Films* **12** 167

[2] Meyer G and Rieder K H 1995 *Surf. Sci.* **331–333** 600
Horn-von Hoegen M, Schmidt T, Meyer G, Winau D and Rieder K H 1995 *Phys. Rev.* B **52** 10764
Smith A R, Chao K-J, Niu Q and Shih C-K 1996 *Science* **273** 226
Paggel J J, Miller T and Chiang T-C 1999 *Science* **283** 1709

[3] Budde K, Abram E, Yeh V and Tringides M C 2000 *Phys. Rev.* B **61** 10 602

[4] Aballe L, Rogero C, Kratzer P, Gokhale S and Horn K 2001 *Phys. Rev. Lett.* **87** 156801

[5] Aballe L, Rogero C and Horn K 2002 *Phys. Rev.* B **65** 125319

[6] Chiang T-C 2000 *Surf. Sci. Rep.* **39** 181 and references therein

[7] Aballe L, Barinov A, Locatelli A, Heun S and Kiskinova M 2004 *Phys. Rev. Lett.* **93** 196103

[8] Guo Y, Zhang Y-F, Bao X-Y, Han T-Z, Tang Z, Zhang L-X, Zhu W-G, Wang E G, Niu Q, Qiu Z Q, Jia J-F, Zhao Z-X and Xue Q-K 2004 *Science* **306** 1915
Özer M M, Thompson J R and Weitering H H 2006 *Nat. Phys.* **2** 173
Eom D, Qin S, Chou M-Y and Shih C K 2006 *Phys. Rev. Lett.* **96** 027005

[9] Parkin S S P, More N and Roche K P 1990 *Phys. Rev. Lett.* **64** 2304
Parkin S S P 1991 *Phys. Rev. Lett.* **67** 3598
Ortega J E and Himpsel F J 1992 *Phys. Rev. Lett.* **69** 844
Ortega J E, Himpsel F J, Mankey G J and Willis R F 1993 *Phys. Rev.* B **47** 1540

[10] Tang S-J, Basile L, Miller T and Chiang T-C 2004 *Phys. Rev. Lett.* **93** 216804
Tang S-J, Lee Y-R, Chang S-L, Miller T and Chiang T-C 2006 *Phys. Rev. Lett.* **96** 216803

[11] Moras P, Ferrari L, Spezzani C, Gardonio S, Ležaić M, Mavropoulos Ph, Blügel S and Carbone C 2006 *Phys. Rev. Lett.* **97** 206802

[12] Matsuda I, Ohta T and Yeom H W 2002 *Phys. Rev.* B **65** 085327

[13] Speer N J, Tang S-J, Miller T and Chiang T-C 2006 *Science* **314** 804

[14] Matsuda I, Woong Yeom H, Tanikawa T, Tono K, Nagao T, Hasegawa S and Ohta T 2001 *Phys. Rev.* B **63** 125325

[15] Chao K-J, Zhang Z, Ebert Ph and Shih C K 1999 *Phys. Rev.* B **60** 4988

[16] Evans D A, Alonso M, Cimino R and Horn K 1993 *Phys. Rev. Lett.* **70** 3483

[17] Jiang C-S, Yu H-B, Wang X-D, Shih C-K and Ebert Ph 2001 *Phys. Rev.* B **64** 235410

[18] Moras P, Theis W, Ferrari L, Gardonio S, Fujii J, Horn K and Carbone C 2006 *Phys. Rev. Lett.* **96** 156401

[19] Babalola I A, Petro W G, Kendelewicz T, Lindau I and Spicer W E 1984 *Phys. Rev.* B **29** 6614
Aristov V Yu, Le Lay G, Thanh Vinh Le, Hricovini K and Bonnet J E 1993 *Phys. Rev.* B **47** 2138
Aristov V Yu, Bertolo M, Althainz P and Jacobi K 1993 *Surf. Sci.* **281** 74

[20] Aristov V Yu, Bertolo M, Jacobi K, Maca F and Sheffler M 1993 *Phys. Rev.* B **48** 5555

[21] Othake A, Nakamura J and Osaka T 1997 *Surf. Sci.* **380** L437

[22] Bohr J, Feidenhans'l R, Nielsen M, Toney M, Johnson R L and Robinson I K 1985 *Phys. Rev. Lett.* **54** 1275